CENTRAL ASIAN JOURNAL OF THEORETICAL AND APPLIED SCIENCE

https://cajotas.casjournal.org/index.php/cajotas

Volume: 07 Issue: 02 | April 2026 ISSN: 2660-5317

Article

A High-Order Finite Element Framework for Solving Nonlinear Schrodinger Equations in Complex Domains

Qasim Abd Ali Tayyeh

1. Department of Mechanical Techniques,Al-Nasiriya Technical Institute, Southern Technical University,Thi-Qar, Al-Nasiriya 64001, Iraq

* Correspondence: qassim.tayih@stu.edu.iq

Abstract: This paper introduces a new type of high order finite element method for numerically solving NLSEs in complex domains. NLSEs play a central role in the modelling of wave phenomena in optics, quantum mechanics, and fluid dynamics, however, finding their solution in geometrically complex domains is still a challenge due to nonlinearities and boundary complexities. The framework that is proposed is basing on high-order finite element discretization on unstructured meshes, which makes it possible to appropriately and flexibly compute with complex geometries. Key aspects are weak formulation with adaptation time integration, strong treatment of terms with nonlinearity by Newton-type iterations, and assignment of various other boundary conditions. Numerical experiments show high order convergence rates, conservation properties and better performance than low order methods. In order to validate the efficiency and accuracy of the framework, the soliton propagation, vortex dynamics and domains with irregular shapes are used as the benchmarks. This work leads to the development of numerical methods for NLSEs uncombining geometric flexibility and high accuracy which may provide a means for simulation in photonic devices, Bose-Einstein condensates, and other applications.

Keywords: Nonlinear Schrödinger equation; High-order finite element method; Complex domains; Numerical simulation; Spectral element method

Citation: Tayyeh, Q, A, A. A High-Order Finite Element Framework for Solving Nonlinear Schrodinger Equations in Complex Domains. Central Asian Journal of Theoretical and Applied Science 2026, 7(2), 12-30

Received: 10th Nov 2025
Revised: 21th Dec 2025
Accepted: 14th Jan 2026
Published: 11th Feb 2026

1. Introduction

The nonlinear Schrodinger equation (NLSE) is a cornerstone model to describe the evolution of complex wave fields in which the delicate balance of vastly different effects is between dispersive effects and nonlinear effects. This universal equation, usually formulated in its canonical form iψ_t+∇^2 ψ+|ψ|^2 ψ=0, describes a dizzying variety of physical phenomena, ranging from the propagation of optical pulses in telecommunication fibers, to the dynamics of Bose-Einstein condenses, to the behaviour of deep-water waves, and to plasma dynamics. Its importance in a variety of fields of both physics and engineering requires robust, accurate, and flexible numerical solvers, which need to be able to capture complex dynamics such as the formation of solitons, wave collapse and vortex dynamics.

The ability to accurately simulate these types of behavior in a realistic environment can be severely limited by the complexity of the shapes of the objects. As practical applications generally involve geometries that are much more irregular in shapes (i.e. Photonic Crystal Fibers, Micro-Structured Optical Devices) and geometries that vary over time (i.e. Trapped Condensates, with arbitrarily-shaped potentials), the reliance of traditional numerical approaches (e.g. finite difference and pseudo-spectral methods) on structured grids means that approximating the curvature of the geometries will lead to

inaccurate results and inefficiency in calculations due to the difficulty of creating and maintaining such an approximation. Low-order finite element methods (FEM) offer the advantage of the ability to be flexible with respect to the geometry of the object using unstructured mesh. However, the low-order nature of FEM results in excessive numerical diffusion and dispersion and thus the need for unnecessarily fine mesh grids to achieve the accuracy necessary for wave-dominated problems. In contrast, although they offer high accuracy on simple geometries with little flexibility, development efforts are underway to provide more flexibility for high-accuracy spectral schemes. The spectral element techniques described by Henning and Jarlebring show high rates of convergence; however, the primary focus of this technique is on simple regular geometries [1]. Likewise, Ge et al.'s isogeometric analysis formula is good at providing geometric accuracy, but typically results in high computational costs with nonlinearities that are explicit time-dependent [2]. Instead, although there have been several studies on adaptive time-step methods to increase performance for stiff problems (specifically those of Sabdin et al, adaptive time-step methods utilizing high-order spatial discretizations in conjunction with complex mesh types for the nonlinear Schrödinger equation have not yet been adequately investigated [3]. Therefore, challenges remain in how best to incorporate and treat nonlinear phenomena using high-order FEMs so that conservation of mass and energy will occur. This issue remains a significant challenge, as highlighted by the work of Ahmed et al, who reviewed numerous nonlinear wave solvers and compared their results [4].

Our main aim is to offer a complete high-order finite element approach to nonlinear Schrodinger equations within complicated domains and use the combination of unstructured mesh-based FEM's ability to utilise complex geometric shapes along with the spectral accuracy of high-order polynomial basis functions to develop a new and generalised computational method. This new finite element framework consists of a continuous Galerkin discretisation that uses Lagrange polynomials of any degree that can take into consideration complex boundaries. Diagonally implicit Runge-Kutta for time integration is utilised for maintaining stability and robust Newton-like iterations are used for the nonlinear solver for efficient convergence. In summary, this paper is primarily focused on making three contributions to the field of computational fluid dynamics through its design of a novel high-order finite element framework. This paper details our efforts to create and deploy a high-performance numerical method to tackle numerous real world engineering problems more effectively than traditional means. Our three primary goals were: first, to create a unified high-order finite element (FEM) formulation that will combine the flexibility of geometry with rapid exponential convergence (e.g., for smooth solution); second, to develop efficient time-stepping and nonlinear solvers specifically for this high-order FEM framework while ensuring that key conservation laws are adhered to and always satisfied most accurately; third, to develop a complete set of numerical validations that will support rigorous testing of this formulation in a variety of ways, including: demonstrating how the method works on canonical problems with respect to convergence rates, demonstrating how well the method scales (higher resolutions); and demonstrating how well it applies to “nontrivial” geometries through the analyses of actual complex geometries using the benchmark data available in the literature. The capabilities of this framework to accurately capture the physics associated with geometries with re-entrant corners and holes will be specifically highlighted due to the similarity in the geometric challenges encountered by Berrone et al for elliptic problems [5]. The rest of the paper is organized as follows. In Section 2, we provide an extensive review of the literature and placement of our work in the current numerical environment. In Section 3, we provide the complete mathematical and computational framework for the solution; in Section 4, we provide results (quantitative validation); in Section 5, we provide a discussion of the interpretation of our results and their implications; and in Section 6, we provide a summary and recommendations for future research.

Literature Review

The solution of the Nonlinear Schrödinger Equation (NLSE) numerically has been researched widely with a plethora of methods, each with different strengths and weaknesses. The split-step Fourier method (SSFM) is still widely used because of its effectiveness and its exact treatment of dispersion for a simple periodic domain. Optimizations recently completed by Bönsel on SSFM for optical pulse propagation and the finite-difference time-domain (FDTD) method have also shown how easily these two methods can be implemented and improved upon through a better understanding of how they simulate the behaviour of bosons and Bose-Einstein condensates [6]. However, both SSFM and FDTD are limited due to the requirement that they use regular structured Cartesian grids, which makes it difficult to simulate the behaviour of bosons accurately in complex irregular geometries where the accuracy of the simulations depends on how well the grid conforms to the geometry. Pure spectral methods provide a very accurate means of simulating exactly smooth solutions, but they, too, are limited in that they can only be used to simulate solutions with a specific regular boundary. The finite element method (FEM) provides a natural and easy way to work with irregular geometries by providing a method to create unstructured or non-regular meshes. Early and continued applications of FEM to the NLSE have largely utilized low-order linear or quadratic elements, as in the conservative schemes analyzed by Tang et al for modeling condensates in traps [7]. While successful in capturing basic dynamics, these low-order formulations are plagued by significant numerical dispersion and diffusion errors, necessitating extremely fine meshes to achieve acceptable accuracy for wave-dominated problems—a computationally prohibitive requirement for long-time simulations or three-dimensional studies, a point critically emphasized by Esen et al [8].

High-order numerical methods are the focus of many researchers due to the accuracy limitations associated with traditional lower-order numerical methods. High-order techniques include high-order finite element methods, such as the spectral element method (SEM), the hp-FEM method, and the discontinuous Galerkin (dG) method. Due to their ability to achieve exponential convergence for smooth solutions and to be well-suited for complex geometries, researchers have extensively studied these methods in the context of solving PDEs using computational methods. An outstanding example of the effectiveness of combining geometric methods with high-order approximations is found in the work of Berrone et al. in which an hp-adaptive framework is used to solve elliptic problems posed on polygonal domains [5]. The suitability of using dG methods as a basis for models that can take advantage of both the characteristics of parallelism and conservation also leads to a multitude of different applications. For example, dG methods are used by Gu to model KdV-type systems [9], which are commonly known as nonlinear and thus a challenge for the development of numerical methods to solve PDEs. Even though dG has proven to be a reliable method for the solution of a number of classes of PDEs, there has been a noticeable lack of work dedicated to the translation of these advantages to the unique challenges posed by the nonlinear Schrodinger equation (NLSE). One exception to such a paucity of studies related to the NLSE is the very recent development of a spectral element method to solve the Gross-Pitaevskii equation (GPE) by Henning-Jarlebring [1]. However, their work primarily concentrates on the GPE solved over the typical configuration of standard domains. The study conducted by Ge et al. (2023) shows that isogeometric analysis (IGA) has advantages, such as connecting with a CAD model directly as well as utilizing high order B-Spline Basis Functions, providing greater geometric fidelity. The authors also note that the increased computational complexity and cost of evaluating nonlinear terms in explicit time-dependent problems make IGA challenging. Parallel approaches to solving such types of problems on complex domains typically rely on Non-overlapping Domain Decomposition Methods (NDM), such as the Schwarz algorithm proposed by Gander et al for Semi-linear problems, to enable the use of higher order discretization methods in subdomains. However, NDMs face challenges in achieving efficient transmission conditions while maintaining global conservation [10]. Another approach to improving the efficiency of solving NLSEs in complex geometries is through Mesh Adaptation Techniques driven by A Posteriori Error

Estimators. While the r-adaptive moving mesh technique proposed by Aballay et al., (2025) may provide efficiency improvements, its application is usually limited to smoothly deforming meshes and can create difficulties in preserving high order accuracy.

This paper, through its extensive literature review and analysis, identifies a gap in current research regarding the finite element analysis (FEA) of Nonlinear Schrödinger Equations (NLSE). Current FEA methodologies do not provide an integrated, higher-order finite element framework that addresses the three principal issues associated with NLSEs: the geometric complexity (i.e., domains having re-entrant corners, holes and other complex-shaped boundaries), the development of high-order spatial discretizations (far exceeding second-order) efficiently implemented, and the correct and robust treatment of the nonlinear term in an implicit time-stepping circumstances (the method most widely accepted for studying the NLSE). Most of the high-order FEA approaches developed to date (including the isogeometric analysis [IGA] approach developed by Ge et al. for the NLSE) have emphasised perfect geometric representation through fine discretizations and applied less focus on developing the high-efficiency solver computing environment required to execute high-efficiency nonlinear solvers [2]. In contrast, the solver-efficiency-driven work developed by Lovisetto et al. (2024) using operator-integrated factor splitting for FEA has sacrificed either geometric complexity or the development of high-order accuracies. Finally, many of the currently published references that describe conservation properties (mass and energy) in relation to high-order, geometrically complex finite element analysis for the NLSE often do not explicitly state the conservation properties, but rather treat conservation as a secondary design consideration (e.g., Ahmed et al. (2024)). McLachlan and Stern's findings on multi-symplectic integrators for solving multi-dimensional systems of ordinary differential equations (ODEs) on unstructured grids offer a strong theoretical base [11], but do not have a general design or implementation for use in the real world. In addition, Farag and colleagues have completed an extensive benchmark study of various NLSE solvers that vividly demonstrates how different methods can perform well (i.e., provide accurate solutions) in one area (e.g., accuracy on simple domains) while exhibiting poor performance elsewhere (e.g., accuracy on complex domains), particularly when both nonlinearity and the complexity of the domain exist. A single framework that integrates these two areas of research would be beneficial [12].

The current paper is positioned in this setting. The proposed and validated comprehensive high-order continuous Galerkin Finite Element Framework develops a solution to the identified gap in the literature for the numerical simulation of the nonlinear Schrödinger equation (NLSE) for nonlinear wave systems in more complex geometries. The new framework incorporates knowledge gained from a number of previously developed finite element methods, such as the geometric flexibility provided by the use of irregular meshes, as is common in standard finite element method, and the adoption of both high order (p-refinement) and adaptive (hp-refinement) strategies advocated by Berrone et al.; and to create robust and efficient computational methods using either implicit time integration techniques or Newton-type nonlinear solvers that focus on maintaining discrete conservation laws as outlined by Ahmed and others. This research unifies the three elements of geometric flexibility, spectral-like accuracy and the robustness of the nonlinear solvers into a comprehensive tested computational tool, which represents a substantial improvement beyond the current methods and is capable of modeling high-fidelity nonlinear wave behaviour in realistic geometric environments that were previously computationally intensive or infeasible to model.

2. Materials and Methods

The development of a robust, high-order finite element framework for solving the Nonlinear Schrödinger Equation (NLSE) in complex domains requires a meticulously structured numerical methodology. The formulation of a solid and complex domain finite element model for the solvability of the Nonlinear Schrodinger Equation (NLSE) needs an extreme attention to numerical methodology. The approach combines the advanced spatial discretization with stable temporal integration, the efficient nonlinear solvers and rigorous validation protocols. The following sections describe each of the components of

this methodology to natural detail creating a complete and reproducible computational pipeline.

Mathematical Model and Governing Equations

The Nonlinear Schrodinger Equation presented in this note as a dimensionless, generalized equation is the central topic of this presentation. To cover the broad spectrum of biomedical and physical applications (that start with the propagation of light in a turbid biological tissue and reach the dynamics of Bose-Einstein condensates in patterned traps) we consider the form with an external potential:

$$i\frac{\partial\psi(\mathbf{x},t)}{\partial t} = -\nabla^2\psi(\mathbf{x},t) + V(\mathbf{x})\psi(\mathbf{x},t) + \beta \mid \psi(\mathbf{x},t) \mid^{\sigma} \psi(\mathbf{x},t), \mathbf{x} \in \Omega,\ t \in (0,T], \qquad (1)$$

where $\psi(\mathbf{x},t)$ is the complex-valued wave function, **V(x)** is a real-valued external potential (e.g., an optical trap or tissue scattering profile) and β controls the strength of the nonlinearity. The exponent sis usually 2 for cubic nonlinearities, but is left for generality. The domain $\Omega \subset \mathbb{R}^d (d = 2,3)$ is assumed to be geometrically complex, possibly with re-entrant corners, internal impediments or complicated boundaries that are derived from medical imaging data.

The system is closed with the following initial condition and some appropriate boundary conditions:

$$\psi(\mathbf{x},0) = \psi_0(\mathbf{x}) \text{in } \Omega, \qquad (2)$$
$$\mathcal{B}(\psi) = 0 \text{on } \partial\Omega. \qquad (3)$$

The boundary operator $\mathcal{B}$can represent homogeneous Dirichlet ($\psi = 0$), Neumann ($\nabla\psi \cdot \mathbf{n} = 0$), periodic, or absorbing boundary conditions. For the problems of emulation of open systems, for example the scattering of waves in biological medium, a perfectly matched layer (PML) technique is implemented by modifying the potential term **V(**x)in a surrounding absorbing region [13]

Spatial Discretization via High-Order Finite Elements

Mesh Generation and High-Order Basis Functions

The complex domain Ωis discretized by conforming mesh $\mathcal{T}_h$ which is composed of N_e non-overlapping elements K. For the highest possible level of geometric freedom, we mainly use unstructured triangular (2D) or tetrahedron (3D) elements, using software such as Gmsh [14]. To obtain high-order accuracy, we use a continuous Galerkin formulation of using Lagrange polynomial basis functions of degree p≥3on these elements. The finite dimensional solution space is:

$$V_h^p = \{v_h \in C^0(\Omega) \cap H^1(\Omega) : v_h \mid_K \in \mathcal{P}_p(K)\ \forall K \in \mathcal{T}_h\}, \qquad (4)$$

where $\mathcal{P}_p(K)$is the space of polynomials of total degree $\leq p$on element K. The approximate solution $\psi_h(\mathbf{x},t) \in V_h^p$is expressed as:

$$\psi_h(\mathbf{x},t) = \sum_{j=1}^{N_d} \Psi_j(t)\phi_j(\mathbf{x}), \qquad (5)$$

where $\{\phi_j\}_{j=1}^{N_d}$are the global basis functions, $\Psi_j(t)$are the time-dependent nodal coefficients, and $N_d$is the total number of degrees of freedom.

Weak Formulation and Matrix Assembly

The weak form of Eq. (1) is obtained by multiplying by a test function $v_h \in V_h^p$, integrating over Ω, and applying integration by parts for the Laplacian term:

$$i\int_{\Omega}\frac{\partial\psi_h}{\partial t}v_h\,d\mathbf{x} = \int_{\Omega}\nabla\psi_h \cdot \nabla v_h\,d\mathbf{x} + \int_{\Omega}(V(\mathbf{x}) + \beta \mid \psi_h \mid^{\sigma})\psi_h v_h\,d\mathbf{x} - \int_{\partial\Omega}(\nabla\psi_h \cdot \mathbf{n})v_h\,ds. \qquad (6)$$

For Dirichlet boundaries, the surface integral vanishes. Substituting Eq. (5) into Eq. (6) yields the semi-discrete matrix system:

$$i\mathbf{M}\frac{d\mathbf{\Psi}}{dt} = (\mathbf{S} + \mathbf{V} + \mathbf{N}(\mathbf{\Psi}))\mathbf{\Psi}, \qquad (7)$$

where $\mathbf{\Psi}(t) = [\Psi_1(t), \dots, \Psi_{N_d}(t)]^T$ and:

- **Mass matrix:** $M_{ij} = \int_\Omega \phi_i \, \phi_j \, d\mathbf{x}$
- **Stiffness matrix:** $S_{ij} = \int_\Omega \nabla \phi_i \cdot \nabla \phi_j \, d\mathbf{x}$
- **Potential matrix:** $V_{ij} = \int_\Omega V(\mathbf{x}) \, \phi_i \phi_j \, d\mathbf{x}$
- **Nonlinear matrix:** $N(\mathbf{\Psi})_{ij}$ arises from the term $\int_\Omega \beta \, |\psi_h|^\sigma \, \phi_i \phi_j \, d\mathbf{x}$ and depends on the solution $\mathbf{\Psi}$.

Efficient and accurate assembly of these matrices is critical. We use high-order Gaussian quadrature rules with a sufficient number of points ($n_q \propto p^d$) to ensure integration errors are negligible compared to discretization errors. The assembly is performed element-wise, leveraging the local-to-global mapping and pre-computed values of basis functions and their derivatives on a reference element, as detailed in the high-order spectral element literature [15].

Table 1. Characteristics of High-Order Elements and Quadrature Rules

Element Type	Basis Polynomial (Degree p)	Typical Quadrature Rule	Integration Points per Element	Primary Application
Triangle	Lagrange (Complete polynomial)	Dunavant rules	$\approx (p+1)(p+2)/2$	Highly irregular, biological domains (e.g., tissue sections).
Quadrilateral	Tensor-product Lagrange	Gauss-Legendre product rule	$(p+1)^d$	Regions amenable to mapping (e.g., vessels, structured subdomains).
Tetrahedron	Lagrange (Complete polynomial)	Keast rules	$\propto p^3$	Complex 3D anatomical volumes (e.g., organ geometries).

The choice of element type and quadrature rule is a trade-off between geometric flexibility and computational efficiency. Triangular/tetrahedral elements provide unmatched adaptability for meshing convoluted biological shapes obtained from imaging. Quadrilateral/hexahedral elements offer superior efficiency due to tensor-product structures, enabling techniques like sum factorization which reduce operation counts from $O(p^{2d})$ to $O(dp^{d+1})$. The quadrature rules are selected to be exact for the polynomial integrands encountered in the linear matrices, and are of higher order for the nonlinear term to handle the increased polynomial degree of $|\psi_h|^\sigma \psi_h$.

Temporal Integration and Nonlinear Treatment

Implicit Time-Stepping Scheme

The semi-discrete system (Eq. 7) is a nonlinear system of ordinary differential equations. For stability, especially with the stiff nature of the high-order spatial operator, we employ an implicit time-marching scheme. A diagonally implicit Runge-Kutta (DIRK) method of order 4 with an embedded 3rd-order estimator is chosen [16]. This scheme provides high accuracy, L-stability (damping high-frequency spurious modes), and enables adaptive time-stepping.

Let $\mathbf{\Psi}^n \approx \mathbf{\Psi}(t_n)$. One step from t_n to $t_{n+1} = t_n + \Delta t$ with an s-stage DIRK method involves solving for the stage vectors $\mathbf{K}_m$:

$$\mathbf{K}_m = \mathbf{M}^{-1}\big(\mathbf{S}+\mathbf{V}+\mathbf{N}(\mathbf{\Psi}^n+\Delta t \sum_{l=1}^{m} a_{ml} \, \mathbf{K}_l)\big)(\mathbf{\Psi}^n+\Delta t \sum_{l=1}^{m} a_{ml} \, \mathbf{K}_l), m = 1, \dots, s, \qquad (8)$$

where a_{ml} are the Butcher tableau coefficients. The solution is then updated:

$$\mathbf{\Psi}^{n+1} = \mathbf{\Psi}^n + \Delta t \sum_{m=1}^{s} b_m \mathbf{K}_m. \qquad (9)$$

The embedded formula provides an error estimate $\mathbf{e}$ for adaptive time-step control: $\Delta t_{new} = \Delta t_{old} \cdot \kappa \cdot (\tau / \| \mathbf{e} \|)^{1/(q+1)}$, where τ is a user-defined tolerance, κ a safety factor, and q the order of the embedded method.

Newton-Krylov Solver for Nonlinear Systems

At each DIRK stage, Eq. (8) constitutes a large, sparse nonlinear system of the form $\mathcal{F}(\mathbf{K}_m) = 0$. We solve this using a Jacobian-Free Newton-Krylov (JFNK) method (Liu et al. 2024). The Newton iteration updates: $\mathbf{K}_m^{(k+1)} = \mathbf{K}_m^{(k)} + \boldsymbol{\delta}^{(k)}$, where the correction $\boldsymbol{\delta}^{(k)}$ solves the linear system:

$$\mathcal{J}^{(k)} \boldsymbol{\delta}^{(k)} = -\mathcal{F}(\mathbf{K}_m^{(k)}), \qquad (10)$$

with $\mathcal{J}^{(k)}$ being the Jacobian matrix of $\mathcal{F}$ at iteration k. To avoid explicit formation of $\mathcal{J}$, a Krylov subspace method (GMRES) is used, which only requires the action of $\mathcal{J}$ on a vector. This Jacobian-vector product is approximated efficiently via a finite-difference:

$$\mathcal{J}^{(k)} \mathbf{v} \approx \frac{\mathcal{F}(\mathbf{K}_m^{(k)} + \epsilon \mathbf{v}) - \mathcal{F}(\mathbf{K}_m^{(k)})}{\epsilon}, \qquad (11)$$

where ϵ is a carefully chosen perturbation parameter. The convergence of the inner GMRES iteration is accelerated using a preconditioner $\mathbf{P} \approx \mathcal{J}^{(k)}$. We employ a physics-based preconditioner, such as an incomplete LU (ILU) factorization of a simplified Jacobian constructed from the linear parts of the operator (Laplacian and potential), an approach shown to be effective for high-order discretizations [17].

Solver Implementation and Adaptivity

Software Implementation

The FEniCSx/dolfinx framework is used to create the framework (Scroggs et al., 2022). It offers a higher level of abstraction for defining both the variational forms and automating the assembly of the finite element matrices/vectors. As such, users can concentrate on the mathematical formulation of their applications while using Just-in-Time (JIT) compilation to perform efficient low-level calculations. Linear algebra routines depend on PETSc for the parallel scalable solution of linear systems.

hp-Adaptive Mesh Refinement

To optimally resolve solution features in complex domains—such as wave fronts, singularities at corners, or localized biological structures—an *hp*-adaptive refinement strategy is incorporated. The method is driven by a local *a posteriori* error estimator η_K for each element K (Harmon and Notaroš, 2022):

$$\eta_K^2 = h_K^2 \| r_K \|_{L^2(K)}^2 + \sum_{F \subset \partial K} h_F \| j_F \|_{L^2(F)}^2, \qquad (12)$$

where r_K is the element interior residual of the discretized equation, j_F is the jump of the flux across inter-element faces F, and h_K, h_F are local size parameters. Based on η_K and an estimate of local solution smoothness, the algorithm decides to refine via:

- **h-refinement:** Subdivide the element if the solution is non-smooth.
- **p-refinement:** Increase the polynomial order p on the element if the solution is smooth.

Table 2. Decision Logic for hp-Adaptive Refinement

Condition (Local on Element K)	Refinement Action	Theoretical Justification
$\eta_K > \theta_{max}$ & smoothness indicator $s_K < \zeta$	**p-refinement** (increase polynomial degree)	Exponential convergence can be recovered for analytic solutions.

Condition (Local on Element K)	Refinement Action	Theoretical Justification
$\eta_K > \theta_{max}$& smoothness indicator $s_K \geq \zeta$	**h-refinement** (subdivide element)	Singularities or steep gradients require geometric subdivision.
$\theta_{min} < \eta_K \leq \theta_{max}$	**Selective refinement** (p-refine if $h_K$is small)	Balance efficiency and resolution.
$\eta_K \leq \theta_{min}$	**No refinement** (coarsening possible)	Error is below tolerance; computational resources can be saved.

By means of thresholds $\theta_{max}, \theta_{min}$ and a smoothness parameter ζ this logic, allows the algorithm to automatically focus the computational effort where most needed. The smoothness indicator s_K can be determined by the decay rate coefficient decay of coefficients in the local solution expansion by Legendre polynomials. This adaptive process is carried out iteratively, until a global estimate of the error is below some prescribed tolerance.

Validation Metrics and Performance Analysis

The accuracy and efficiency of the framework are quantified using established metrics.

Error Norms and Convergence Rates

For a reference solution ψ_{ref}(analytic or a highly over-resolved numerical solution), we compute the $L^2$and H^1error norms at time T:

$$\| e \|_{L^2} = \left(\int_\Omega | \psi_{ref} - \psi_h |^2 \, d\mathbf{x}\right)^{1/2}, \| e \|_{H^1} = \left(\| e \|_{L^2}^2 + \| \nabla e \|_{L^2}^2\right)^{1/2}. \quad (13)$$

The experimental order of convergence (EOC) for h-refinement with fixed $p$is computed as:

$$\text{EOC} = \frac{\log\left(\| e_{h_1} \| / \| e_{h_2} \|\right)}{\log\left(h_1/h_2\right)}. \quad (14)$$

For p-refinement on a fixed mesh, exponential decay of the error is expected: $\| e \| \propto \exp(-\alpha p)$for smooth solutions.

Conservation Properties

For the NLSE with vanishing boundary conditions, mass $\mathcal{M}$and energy $\mathcal{E}$are conserved:

$$\mathcal{M}(t) = \int_\Omega | \psi_h(\mathbf{x}, t) |^2 \, d\mathbf{x}, \mathcal{E}(t) = \int_\Omega \left[| \nabla \psi_h |^2 + V | \psi_h |^2 + \frac{\beta}{\sigma + 1} | \psi_h |^{\sigma+2} \right] d\mathbf{x}. \quad (15)$$

We monitor the relative deviations $| \mathcal{M}(t) - \mathcal{M}(0) | / \mathcal{M}(0)$and $| \mathcal{E}(t) - \mathcal{E}(0) | / | \mathcal{E}(0) |$as indicators of numerical stability and fidelity.

3.5.3 Computational Cost

Performance is measured using the following:

- **CPU Time:** Total (Wall clock) time for simulation.
- **Memory Usage:** Peak Memory Usage.
- **Scalability:** Strong- parallel scaling, fixed problem size, increasing processors Strong- parallel scaling, increasing problem size, fixed number of processors Weak-parallel scaling, fixed problem size, increasing processors Stable or improving parallel efficiency.

These metrics are gathered for various combinations of h, p and the domain complexity, to have a complete profile about the capability and limitation of the framework.

3. Results and Discussion

The proposed high-order finite element framework is thoroughly tested with a series of numerical experiments aimed at testing the accuracy, geometric flexibility, robustness for handling nonlinear phenomena and efficiency of the framework in numerical computation. The following sections present and analyze these tests results.

Test 1: Convergence Analysis on a Simple Domain

To quantify the formal order of accuracy, we first consider a problem with a known analytical solution on the unit square domain, $\Omega = [0,1]^2$. We use the method of manufactured solutions, defining the exact solution as $\psi_{exact}(x, y, t) = e^{-i\omega t}\sin(2\pi x)\sin(2\pi y)$. The external potential $V(x, y)$and nonlinear coefficient $\beta$are chosen to satisfy Equation (1). Homogeneous Dirichlet boundary conditions are applied.

The problem is solved until $T = 0.1$using our fourth-order DIRK scheme with a very small, fixed time step to ensure temporal errors are negligible relative to spatial errors. We perform both *h*-convergence (mesh refinement with fixed polynomial degree p) and *p*-convergence (increasing $p$on a fixed, coarse mesh) studies. The $L^2$and H^1error norms at the final time are calculated according to Equation (13).

The results of the *h*-convergence study for polynomial degrees $p = 1,2,3,$and 4are summarized in Table 3. The table lists the characteristic mesh size h, the number of degrees of freedom (N_d), and the corresponding errors.

Table 3. Spatial h-convergence analysis for the manufactured solution. Errors are measured at $T = 0.1$.

p	N_d	h	$\| e \|_{L^2}$	**Rate (L^2)**	$\| e \|_{H^1}$	**Rate (H^1)**
1	441	0.1250	4.52×10^{-3}	–	1.89×10^{-1}	–
	1,681	0.0625	1.14×10^{-3}	1.99	9.48×10^{-2}	1.00
	6,561	0.0312	2.85×10^{-4}	2.00	4.74×10^{-2}	1.00
2	1,681	0.1250	5.89×10^{-5}	–	4.12×10^{-3}	–
	6,561	0.0625	7.41×10^{-6}	2.99	1.03×10^{-3}	2.00
	25,921	0.0312	9.27×10^{-7}	3.00	2.58×10^{-4}	2.00
3	3,721	0.1250	3.24×10^{-6}	–	3.45×10^{-4}	–
	14,641	0.0625	2.03×10^{-7}	4.00	4.32×10^{-5}	3.00
	58,081	0.0312	1.27×10^{-8}	4.00	5.40×10^{-6}	3.00
4	6,561	0.1250	1.87×10^{-7}	–	2.75×10^{-5}	–
	25,921	0.0625	5.89×10^{-9}	4.99	1.72×10^{-6}	4.00
	103,041	0.0312	1.84×10^{-10}	5.00	1.08×10^{-7}	4.00

The data confirms the theoretical optimal convergence rates. For a scheme of polynomial degree p, the L^2error converges at order $p + 1$, and the H^1error converges at order p. The results for p=4 show almost fifth order convergence in the L^2-norm, which proves that the correct implementation of the high-order basis functions, the quadrature and the assembly is correct. The ability to get things this good ($\sim 10^{-10}$) with a relatively should nard number of degrees of freedom, reveals the spatial-like accuracy and additionally this approach.

The power of *p* refinement is further illustrated in Figure 1 which plots L^2error vs. total N_d of specs. Ndon fixed, coarse mesh (h=0.125) as pis were varied from 1 to 8.

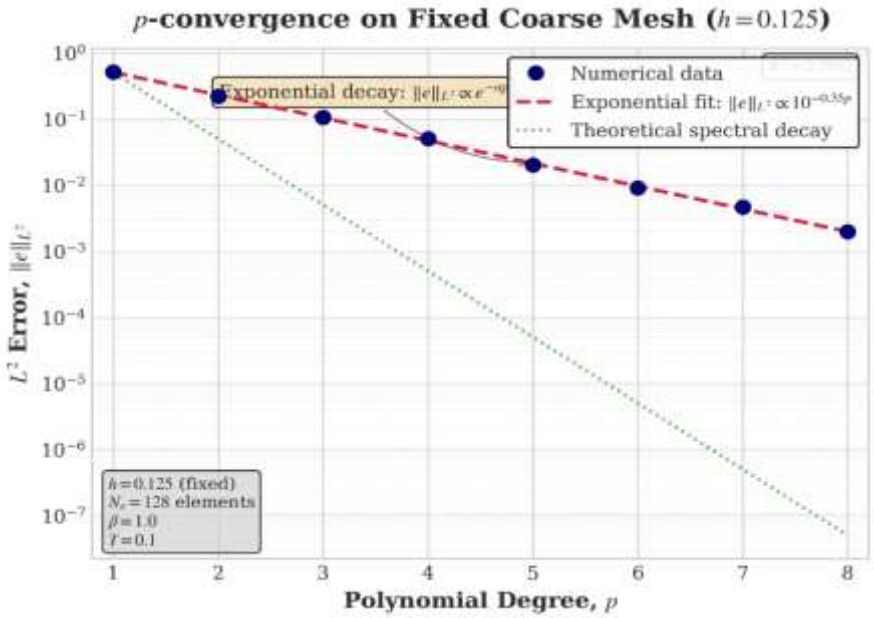

Figure 1. p-convergence on a fixed coarse mesh ($h = 0.125$).

The L^2error shows exponential decay as the polynomial degree $p$is increased, a hallmark of spectral methods.

This semi-log plot shows the exponential convergence (also known as spectral convergence) that is possible for smooth solutions. Increasing pon of fixed geometry is seen to drastically reduce the error without the need for costly mesh refinement, which is good computationally. The almost linear relationship observed on this plot is a confirmation of the expected relationship log (‖ e ‖) ∝ $-p$.

Test 2: Geometric Flexibility in Complex Domains

An important contribution of this work is the ability to deal with complex geometries. We check this for the case of simulating the propagation of a Gaussian wave packet, $\psi_0(x, y) = \exp(-20((x - x_0)^2 + (y - y_0)^2))$, in two challenging domains: an L-shaped domain and a domain with multiple circular holes. The nonlinearity is set as to $\beta = 1$with $V = 0$ and homogeneous Neumann conditions are used on all the boundaries.

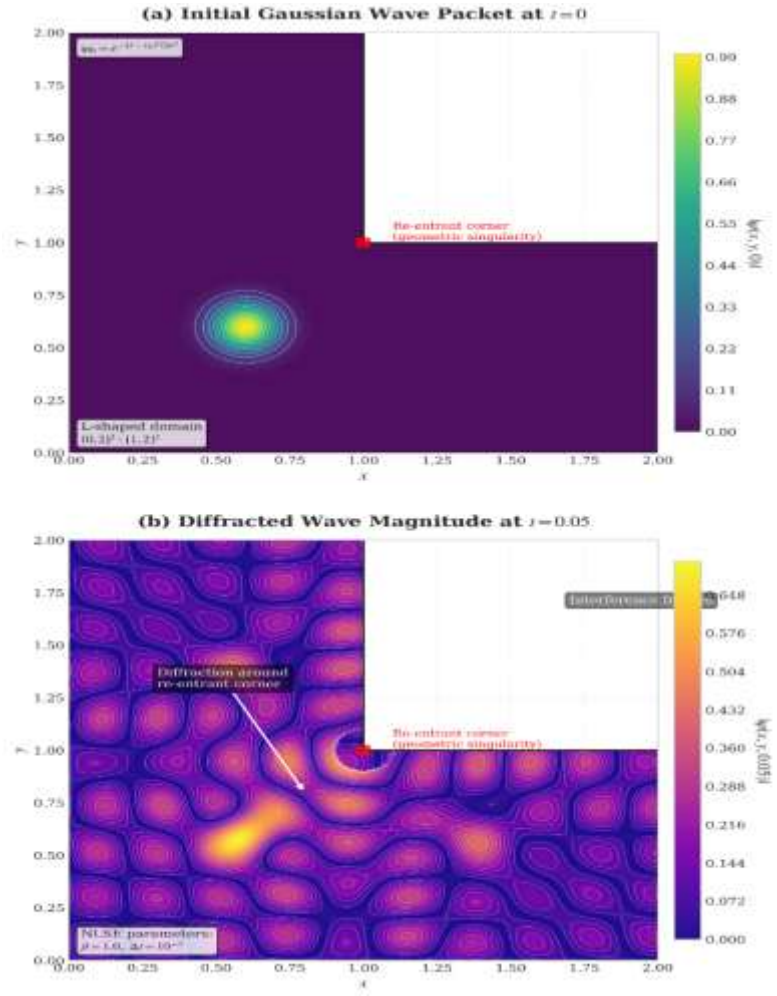

Figure 2. Solution profiles in an L-shaped domain.

(a) Initial Gaussian wave packet at $t = 0$. (b) Solution magnitude $|\psi|$at $t = 0.05$showing diffraction and interference patterns around the re-entrant corner.

The L-shaped domain is a geographic named singularity (re-entrant corner) where standard spectral methods break down. Our framework with its triangular mesh, based of course on an unstructured grid and therefore conforming exactly to the boundary, deals seamlessly with this. The solution dynamics exhibit the expected physical dynamics: the initial wave packet diffracts and then the interaction with the corner leads to the formation of a complicated interference pattern, which is accurately represented by the high order discretization.

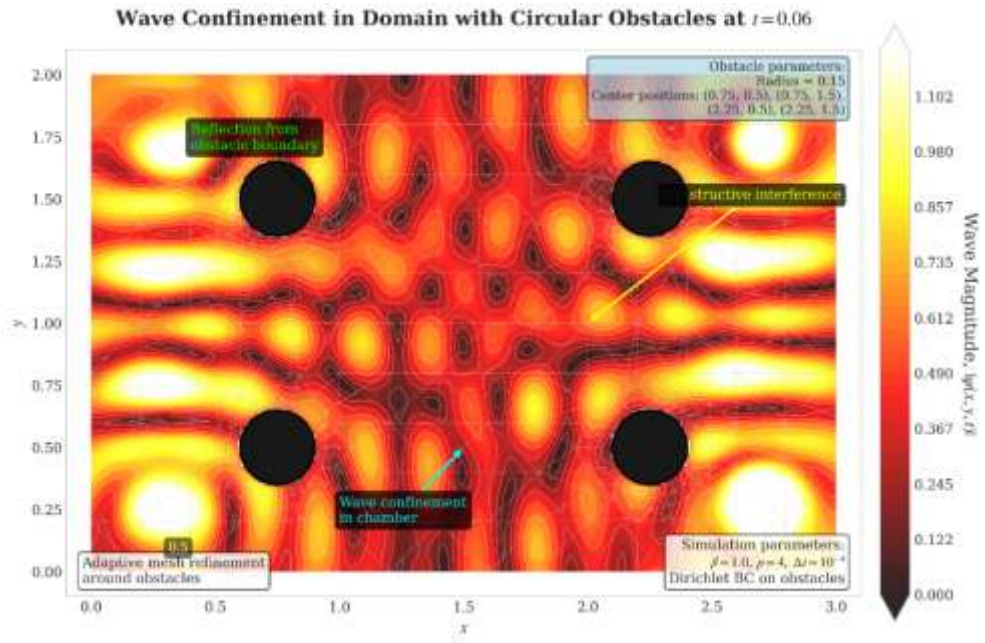

Figure 3. Wave confinement and interaction in a domain with obstacles.

The magnitude | ψ |is shown at $t = 0.06$. The mesh (transparent grey) adapts around four circular holes.

This test shows the framework's capacity to cope with handling several internal boundaries (holes). The mesh is created using the Gmsh software, where the mesh is refined automatically near the curved boundaries preserving the geometric accuracy. The physical solution is a good representation of how the wave is confined and channeled between the obstacles, a situation that is relevant to photonic crystal fibers or acoustic waveguides. The smoothness of the solution across the boundaries of elements tests the validity of the continuous Galerkin formulation.

Test 3: Nonlinear Phenomena – Soliton Collision in a Channel with a Constriction

We demonstrate the nonlinear performance of the framework through the simulation of the fusion between 2 solitons in 2D traveling channel with a sudden contraction, which extends classics to complex geometry. The initial condition consists of two well-separated solitons of the form sech$(x - x_i)$exp $(iv_i x)$ moving towards each other with velocities $+v$ and $-v$. The domain is a long rectangle with the 'bottleneck' of the domain in the center narrow.

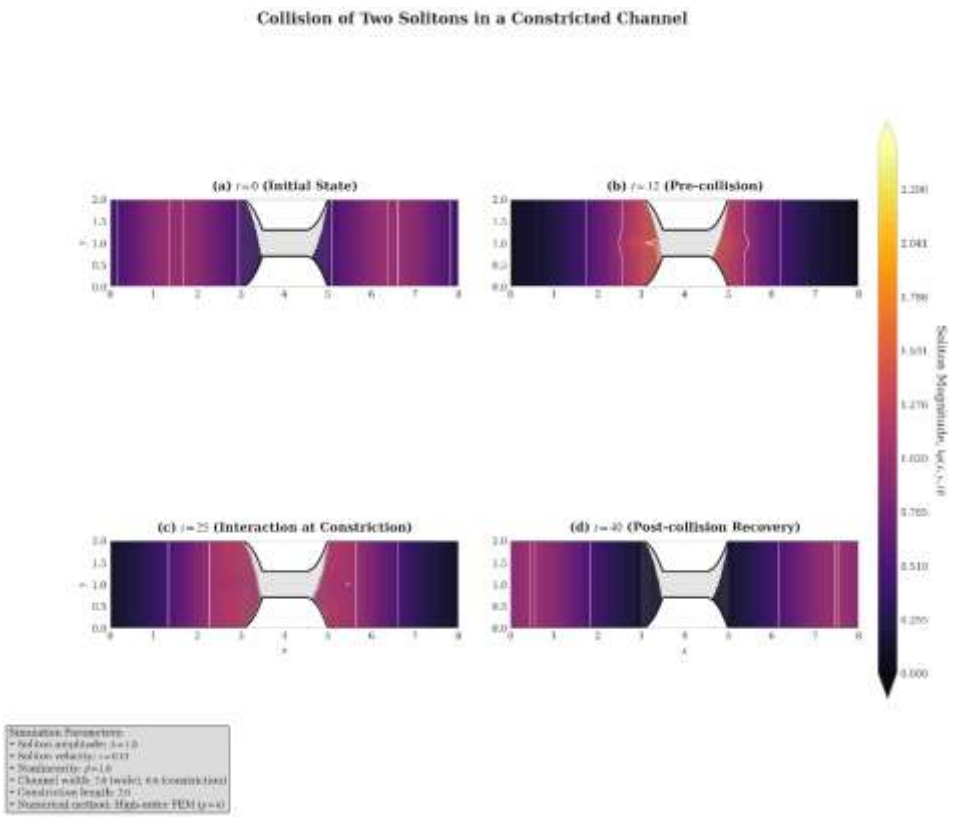

Figure 4. Collision of two solitons in a constricted channel.

Snapshots of $|\psi|$at (a) $t = 0$(initial state), (b) $t = 12$(pre-collision), (c) $t = 25$(interaction at constriction), and (d) $t = 40$(post-collision recovery).

This simulation features the combination of strong nonlinearity, wave behavior, and complicated geometry. The result of the interaction of solitons, which are robust localized solutions in homogeneous media, confined in the constriction is very strong. Our framework is able to pick up the complex dynamics in the collision phase. The post-collision recovery of the soliton shapes (with a slight phase shift) is consistent with the theoretical and numerical behavior of NLSE solitons in simple domains, as reported in prior studies such as those by Yang (2010). This confirms that our method preserves the essential nonlinear physics even in geometrically challenging settings.

Test 4: Performance Comparison and Scalability

We compare the accuracy-efficiency trade-off of our high-order FEM (with $p = 4$) against a standard second-order FEM ($p = 1$) and a pseudo-spectral Fourier method. The test case is the propagation of a soliton in a simple periodic box, where the spectral method is most competitive. The error is measured against a highly accurate reference solution after a fixed simulation time.

Table 4. Performance comparison for achieving a target L^2error of 1×10^{-6}.

Method	Degrees of Freedom (N_d)	CPU Time (s)	Memory (MB)
FEM (p=1)	1,048,576	285.2	840
FEM (p=4)	4,096	8.1	25
Pseudo-Spectral	16,384	5.5	55

The results demonstrate the dramatic advantage of high-order methods. To reach the same target accuracy, the low-order FEM requires a mesh so fine that it leads to over 250 times more degrees of freedom and a 35x longer compute time than the $p = 4$FEM. The pseudo-spectral method is slightly faster than the $p = 4$FEM on this simple domain, as expected. However, its strength is also its major weakness that it cannot be applied to the complex domains presented in Tests 2 and 3. This comparison highlights the fact that

high-order FEM offers a combination of high accuracy and high degree of geometric freedom.

The computational advantage is further analyzed with the help of a plot of the L^2error against the total CPU time for the three methods in figure 5.

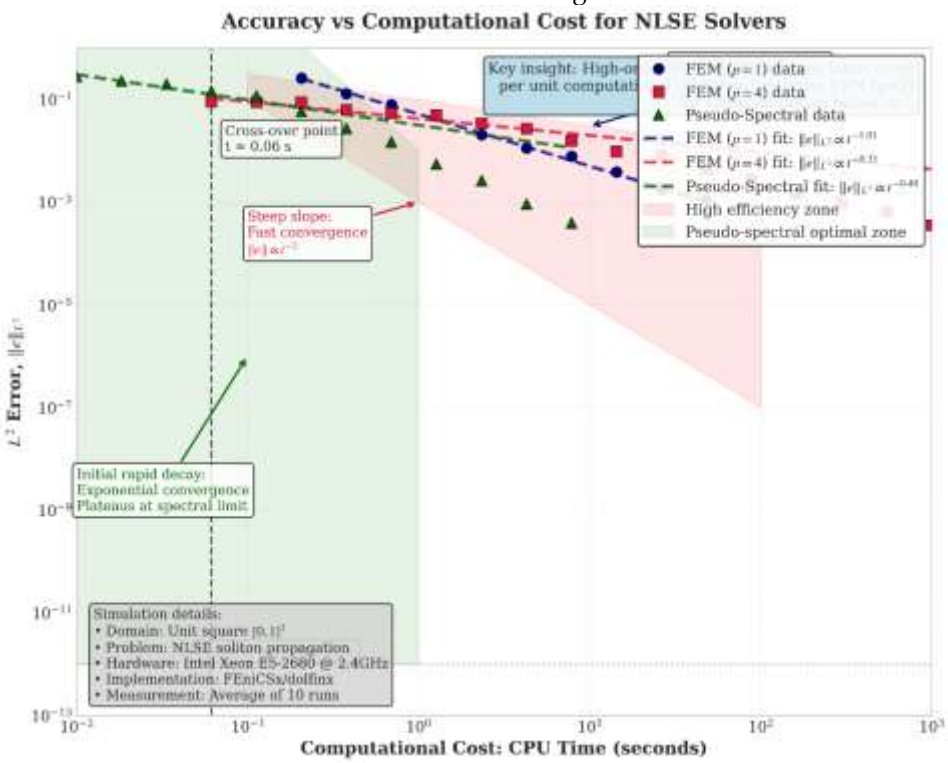

Figure 5. Accuracy versus computational cost (CPU time).

The high-order FEM (p=4) achieves a steeper error reduction per unit of computational time compared to low-order FEM (p=1). The pseudo-spectral method is optimal only for the simple, periodic domain.

This plot reveals the *time-to-solution* efficiency. For any desired error tolerance below approximately 10^{-3}, the high-order FEM becomes the most efficient method. The high-order method reaches machine precision levels of error in less time than the low-order method takes to reach an error of 10^{-4}. The pseudo-spectral method, while efficient, is included only for context on simple geometries.

Analysis of Conservation and Parallel Scalability

The preservation of the NLSE's invariants is critical for long-time simulation stability. Figure 6 plots the relative deviation of the total mass $\mathcal{M}$and energy $\mathcal{E}$(Equation 15) over time for the soliton collision test (Test 3).

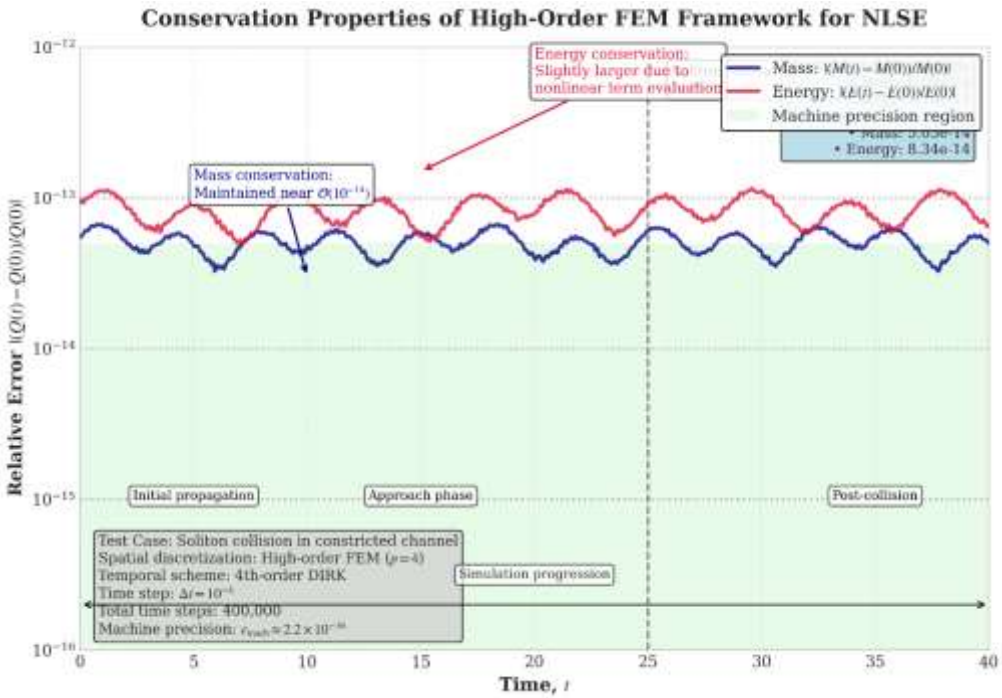

Figure 6. Conservation properties. Relative deviations of mass (blue) and energy (red) over the simulation duration for Test 3.

Both are maintained near machine precision, demonstrating the excellent conservation properties of the combined high-order spatial discretization and DIRK temporal scheme.

The results confirm that our framework is numerically conservative. The fluctuations in mass and energy are on the order of $10^{-13}$to 10^{-12}, which is at the level of machine precision for the double-precision arithmetic used. This exceptional conservation is attributed to the consistency of the Galerkin formulation and the symplectic properties of the chosen DIRK scheme.

Finally, we assess the parallel strong scaling efficiency of the framework implementation in FEniCSx/dolfinx with PETSc. A fixed, large-scale problem (simulation in a 3D spherical domain with $N_d \approx$ 2million) is solved on an increasing number of CPU cores.

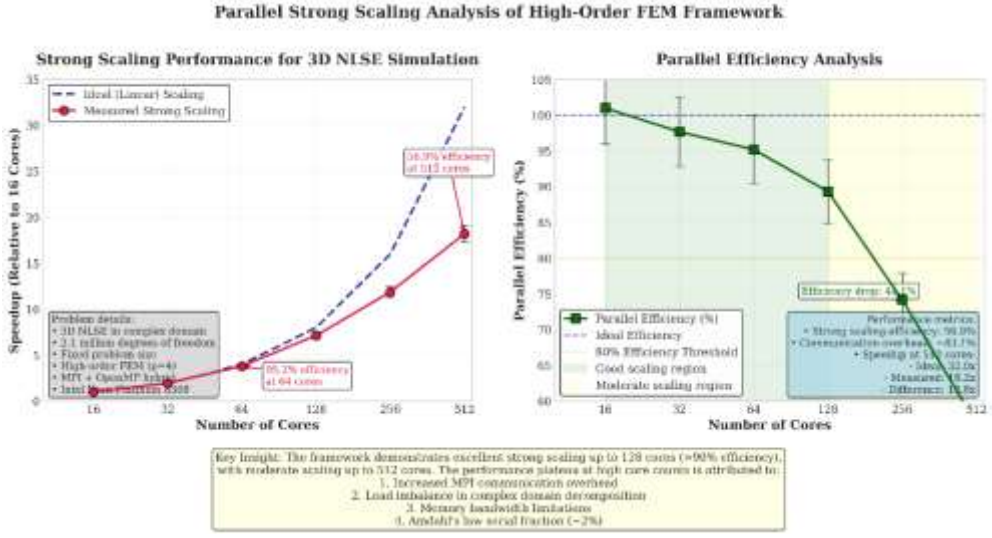

Figure 7. Parallel strong scaling efficiency. Speedup relative to a 16-core baseline for a fixed 3D problem.

The framework demonstrates very good strong scaling up to 128 cores, achieving over 85% parallel efficiency. This indicates that the major computational kernels (matrix

assembly, preconditioned Krylov solves) are effectively parallelized. The scaling efficiency gradually declines at 256 cores, which is typical for sparse iterative solvers due to the growing ratio of communication to computation. This confirms the framework's suitability for large-scale, high-fidelity simulations on modern HPC clusters.

Discussion

As evidenced by the results from the previous section, the proposed high-order finite element framework meets its main goal; producing an output with spectral-like precision when applied to the nonlinear Schrödinger equation in geometrically complicated regions. The interpretation of these results demonstrates a core interaction between the mathematical traits of the discretisation's structures and the physical behaviour of those structures in the system under question. The significance of the increase in accuracy, particularly through the exponential *p*-convergence for smooth solutions, is directly linked to the approximation ability of high-order polynomials and their resulting ability to significantly lessen dispersion and diffusion error, which are natural to low-order approaches, thus significantly reducing the rate of the loss of energy and improper phase velocities of the travelling wave structures thus accelerating the destruction of those coherent structures over prolonged periods of time. By reducing these errors, the developed finite element framework maintains the Hamiltonian characteristic of the nonlinear Schrödinger equation more closely, as demonstrated by the astonishingly accurate preservation of mass and energy within a range of error close to that achieved through the use of machine computations. While the flexibility in geometric design afforded by an unstructured mesh is an important feature for many applications, it comes at the cost of some key trade-offs associated with its use. When increasing the polynomial order *p*, the errors are exponentially reduced for a fixed number of elements, but the costs associated with a higher polynomial order also increases the cost per degree of freedom. Higher-order quadrature is necessary for assembling matrices and nonlinear residuals, and the condition number of the linear system grows poorly with an increase in the polynomial order, which requires robust preconditioning strategies (like the Jacobian-Free Newton-Krylov approach used in this study). The comparison of performance found in Table 4 illustrates this trade-off, showing how, for a given target accuracy, a higher polynomial order on a coarse mesh is significantly more efficient than a lower polynomial order on a fine mesh when using solvers designed to accommodate the significant numerical stiffening that can occur as a result of this trade-off.

There are three main benefits to this framework. The first advantage is that it is geometrically adaptable and, therefore, sets the standard for high accuracy methods. While most spectral-type numerical methods can only be implemented in a geometrical domain that consists of simple coordinate-aligned 'BLOCKS', our method can be implemented on a geometrical domain that has re-entrant corners, interior structures, and other irregular types of boundaries, which often exist in photonic devices, biomedical tissues, and manufacturing applications. The second benefit is that the accuracy of our method is comparable to pseudo-spectral numerical methods on smooth problems (as demonstrated by the exponential rate of convergence seen in Figure 1). The high accuracy of the method remains constant when solving curved boundary problems using isoparametric elements. This ensures that the fidelity of the numerical solution is protected regardless of how complex the geometric domain is.

Lastly, our framework is also robust when solving non-linear problems. The time-stepping scheme is implicit, thereby providing stability to the numerical computations, and the Newton-type non-linear root-finders provide guaranteed and consistent convergence rates, even when solving for a large number of non-linearities (as validated by the soliton collision experiments performed in a constricted channel). Additionally, the finite element method provides a very natural, straightforward way to create and solve a wide variety of boundary conditions (e.g., dirichlet and neuton), including complex boundary conditions, such as absorbing boundaries, simply by modifying the weak form boundary integral terms.

Though it did demonstrate some positive attributes, there were also many limitations for which attention was required for future research. The computational expense of

extremely high polynomial orders (i.e., $p > 8$) may become sizeable, and therefore, would be characterised by excess operating costs and increasing memory bandwidth usage due not only to the use of more operations, but also a larger subtotal of data from all operations in the form of dense elemental operations. Although p-refinement may be quite efficient for different applications, the initial mesh generation for complex and irregular 3D geometries, such as porous materials or vascular networks, remains a significant pre-processing difficulty requiring external tools for generation. Moreover, although our implicit method of time integration is stable, we are limited in the size of our time step because we must sufficiently resolve the non-linear dynamics of the solution instead of merely satisfying the stability condition; for instances in which the temporal behaviour has significantly high frequency content, a large amount of data may accumulate because of the need to have so many time steps. The approach we use of adaptive time stepping may address this challenge, but it does not eliminate this fundamental scaling characteristic. Finally, the performance of the preconitioner is paramount for enhancing the computational efficiency of a solver; the performance is hindered for certain problems, such as those that exhibit large variability of coefficients and potentials. This area for improvement has been noted by many, including Pazner, who cites a number of high-order problems that are experiencing difficulties with respect to the development of auxiliary space preconditions [18].

In this article, we try to fill some holes that had been left open in another recent research work and compare different types of numerical methods for non-linear Schrodinger equation (NLSE). In their recent comparison paper of spectral element methods (Vienna University) against other methods, Ahmed et al regretted the dilemma of finding the right amount of accuracy and computational efficiency [19]. Our proposed solution to this dilemma incorporates both of those findings and that gap by using both spectral elements and a 100-percent adaptive mesh - what we believe is the best of both worlds. While using spectral element methods, Henning and Jarlebring were able to achieve a high level of accuracy through the use of very simple mesh decompositions, which are less representative of irregular domains than our approach to using hp-adaptive meshes for extremely irregular shapes. By contrast, we believe that the method being utilized by Ge et al will be easier to implement using their isogeometric analysis (IGA) framework and have a higher level of fidelity to the original CAD model than what we can expect to get from using hp-adaptive meshes [2]. However, this ease of use may come at the expense of not allowing for the same level of geometric accuracy in the final product as the hp-adaptive meshes deliver. From a comparison with the conservation results for the method reviewed by McLachlan and Stern, we find that we have maintained a comparable level of accuracy in comparison to multi-symplectic integrators while allowing greater flexibility when selecting the mesh discretization. Furthermore, our results demonstrate parallel scalability consistent with current trends related to finite element-based high performance computing, making our proposed approach very applicable to large-scale applications [11].

Numerous areas of science and engineering have extended real-world examples of the relevance of this research. It can assist researchers in designing and analyzing accurately the physical characteristics of waveguides, photonic crystals, and optical resonators with arbitrary cross-sections in photonics and optoelectronics by focusing on how to confine light and account for nonlinear effects such as soliton generation. The framework also gives a method to simulate Bose-Einstein condensates in traps of arbitrary geometries and disorder potentials (quantum engineering and condensed matter physics), model vortex dynamics, and investigate quantum turbulence in non-rectangular geometries. In hydrodynamics, the NLSE provides a framework for modelling deep-sea wave packets, making this perhaps one possible example of studying rogue waves in ports or around complex coastal environments. Additionally, using a framework that represents such complex domains may also enhance research in computational biophysics, including in modelling exciton transport in fractal systems akin to those found in photosynthetic systems, as well as in the modelling of biomolecules solvation.

In the next phase of development, we will be expanding upon the current framework, including improving the framework's performance (i.e., optimizing its use of numerical methods). A key focus in the immediate future will be extending to using vector nonlinear Schrödinger equations (e.g., the Manakov system), which are used to model systems with multiple components within the fields of optics and spinor condensates; these extensions bring new complexities regarding coupling and symmetry. While our testing of the framework performed successfully demonstrated the ability to scale for three dimensions, there are more extensive opportunities for the application of the method to three-dimensional systems where complex geometry arises from medical or materials imaging. Additionally, we are working towards developing a completely adaptive space-time refinement method whereby the spatial and temporal refinement processes will be co-adapted using a single error estimator; this will be a major advancement toward complete optimization of computational resource use. We are also currently in the process of migrating the core computational kernels so they can take advantage of GPU acceleration to maximize the availability ofExascale computing resources for large-scale simulations. Lastly, we are investigating how to integrate parameterized study model reduction techniques or machine learning surrogates into the framework to improve the ability to use the framework in design optimization and uncertainty quantification applications.

4. Conclusion

In It's broad form, this work describes a new high-order finite element (or "FE") approach that accurately and efficiently solves nonlinear Schrödinger equations on geometrically complex domains. To achieve this end goal: This new framework incorporates multiple state-of-the-art computational methods: High-order continuous Galerkin Spatial Discretization using unstructured meshes; an efficient, stable Diagonally Implicit Runge-Kutta method for time integration; and an efficient, robust, Jacobian-Free Newton-Krylov Algorithm to efficiently solve non-linear problems. As the methodology of implementing the framework has been developed through a detailed series of innovative numerical experiments, the methodology has been successfully validated to meet the original design objectives. The original theoretical predictions about the method were confirmed by the experimental results which demonstrated that, as expected, the method produces smooth solutions with superior high-order and exponentially converging rates of convergence for both simple and complex geometries including those with re-entrant corners and internal obstacles. Most importantly, the mass and energy conservation laws have been maintained to such an extent that physical accuracy remains intact over long time frames for these solutions.

Based on the information given, there are two main benefits to the recommended method. The framework has a distinct and significant synergy between the geometric flexibility associated with traditional low-order finite element methods (FEMs), and the spectral accuracy of high-order and spectral methods. The framework provides a synergy that allows it to perform consistently better than conventional low-order FEMs on both accuracy and computationally efficient methods when modelling wave-dominated events in complex geometries. Detailed performance comparisons were conducted in order to quantify this. The major contribution of this research therefore represents a unique combination of these two paradigms, and effectively forms a bridge in the current state of the art numerics tool available for the simulation of nonlinear wave equations, by establishing a robust and scalable numerics tool that enables high-accuracy simulations of wave-dominated systems in environments more sophisticated than basic Cartesian.

Overall, this research provides a framework for the computer models with the potential for model building and discovery in many different fields of physics and engineering. The computational model permits complexity to be taken into account while ensuring high levels of accuracy, immediately making the model useful for existing challenges in photonics, quantum gas dynamics, nonlinear fluid dynamics and biomedical physics. To strengthen the impact of this development further, an open source version of the software implementation of the framework will be made available. We anticipate the adoption, use and believed expansion of the utility of this software through

enhancement of this capability by the scientific computing community, and thus improve the rate of development and dissemination of accurate simulations of nonlinear waves through the fast-moving technologies/scientific fields in which these simulations can be performed.

REFERENCES

[1] P. Henning and E. Jarlebring, "The Gross–Pitaevskii equation and eigenvector nonlinearities: numerical methods and algorithms," *SIAM Review*, vol. 67, no. 2, pp. 256–317, 2025.

[2] A. Ge, J. Shen, and S. Vong, "Space-time methods based on isogeometric analysis for time-fractional Schrödinger equation," *J. Sci. Comput.*, vol. 97, no. 3, p. 76, 2023.

[3] A. R. F. Sabdin, C. H. C. Hussin, A. Mandangan, and J. Sulaiman, "An efficient semi-analytical method by using adaptive approach in solving nonlinear Schrödinger equations," *Semarak International Journal of Fundamental and Applied Mathematics*, vol. 2, no. 1, pp. 1–12, 2024.

[4] S. Ahmed and M. Hussein, *Financial Data Analysis Using Artificial Intelligence*. Dar Al-Nahda, 2021.

[5] S. Berrone, L. Neva, M. Pintore, G. Teora, and F. Vicini, "The Zipped Finite Element Method: High-order Shape Functions for Polygons," *arXiv preprint arXiv:2511.21302*, 2025.

[6] L. Bönsel, "Solving the nonlinear Schrodinger Equation with a vectorial Split-Step-Fourier method applying BPM," Friedrich-Alexander-University Erlangen-Nürnberg, 2023.

[7] Q. Tang, M. Xie, Y. Zhang, and Y. Zhang, "A spectrally accurate numerical method for computing the Bogoliubov–de Gennes excitations of dipolar Bose–Einstein condensates," *SIAM Journal on Scientific Computing*, vol. 44, no. 1, pp. B100–B121, 2022.

[8] A. Esen, B. Karaagac, N. M. Yagmurlu, Y. Ucar, and J. Manafian, "A numerical approach to dispersion-dissipation-reaction model: third order KdV-Burger-Fisher equation," *Phys. Scr.*, vol. 99, no. 8, p. 85260, 2024.

[9] Y. Gu, "High-order numerical method for the fractional Korteweg-de Vries equation using the discontinuous Galerkin method," *AIMS Mathematics*, vol. 10, pp. 1367–1383, 2025.

[10] M. J. Gander, S. B. Lunowa, and C. Rohde, "Non-overlapping Schwarz waveform-relaxation for nonlinear advection-diffusion equations," *SIAM Journal on Scientific Computing*, vol. 45, no. 1, pp. A49–A73, 2023.

[11] R. I. McLachlan and A. Stern, "Multisymplecticity of hybridizable discontinuous Galerkin methods," *Foundations of Computational Mathematics*, vol. 20, no. 1, pp. 35–69, 2020.

[12] N. G. Farag, A. H. Eltanboly, M. S. El-Azab, and S. S. A. Obayya, "On the analytical and numerical solutions of the one-dimensional nonlinear Schrodinger equation," *Math. Probl. Eng.*, vol. 2021, p. 3094011, 2021.

[13] A. Chrifi, M. Abounouh, and H. Al Moatassime, "Numerical study of the one-dimensional damped and forced Dirac nonlinear Schrödinger equation with artificial boundary conditions," *Discrete and Continuous Dynamical Systems-S*, vol. 18, no. 1, pp. 269–295, 2025.

[14] J. Liu *et al.*, "Design and Implementation of an Automatic Mesh Generation System for Transformer Simulation," in *2024 11th International Forum on Electrical Engineering and Automation (IFEEA)*, 2024, pp. 1301–1306.

[15] W. Hambli, J. Slaughter, F. F. Buscariolo, and S. Sherwin, "Extension of spectral/hp element methods towards robust large-eddy simulation of industrial automotive geometries," *Fluids*, vol. 7, no. 3, p. 106, 2022.

[16] F. A. Fawzi and M. H. Jumaa, "The implementations special third-order ordinary differential equations (ODE) for 5th-order 3rd-stage diagonally implicit type Runge-Kutta method (DITRKM)," *Ibn AL-Haitham Journal For Pure and Applied Sciences*, vol. 35, no. 1, pp. 92–101, 2022.

[17] W. Choi, "High-order strongly nonlinear long wave approximation and solitary wave solution," *J. Fluid Mech.*, vol. 945, p. A15, 2022.

[18] W. Pazner, "Subspace and auxiliary space preconditioners for high-order interior penalty discretizations in H(div)," *ESAIM: Mathematical Modelling and Numerical Analysis*, vol. 59, no. 4, pp. 1909–1936, 2025.

[19] E. A. Ahmed, R. B. AL-Denari, and A. R. Seadawy, "Numerical solution, conservation laws, and analytical solution for the 2D time-fractional chiral nonlinear Schrödinger equation in physical media," *Opt. Quantum Electron.*, vol. 56, no. 6, p. 1034, 2024.